IJBPAS, March, 2025, 14(3): 1710-1734

ISSN: 2277–4998

International Journal of Biology, Pharmacy and Allied Sciences (IJBPAS)

'A Bridge Between Laboratory and Reader'

www.ijbpas.com

EXPLORING THE MOLECULAR FRONTIER: VIRTUAL QUEST FOR NOVEL DUAL INHIBITORS TARGETING COX-2 AND 5-LOX

DIVYA V*[1], NAIR AS[1], ACHUTHA AS[1], PUSHPA VL[2] AND MANOJ SV[2]

1: Department of Chemistry, Milad-E-Sherief Memorial College, Kayamkulam, University of Kerala, Kerala, PIN 690502, India

2: Sree Narayana College, Kollam, University of Kerala, Kerala, Kerala, PIN: 691001, India

***Corresponding Author: Dr. Divya. V: E Mail: divyarajiv001@gmail.com**

Received 18th Nov. 2023; Revised 19th Dec. 2023; Accepted 26th May 2024; Available online 1st March 2025

https://doi.org/10.31032/IJBPAS/2025/14.3.8828

ABSTRACT

COX-2/5-LOX dual inhibitors represent an innovative strategy in the development of nonsteroidal anti-inflammatory drugs (NSAIDs). These compounds simultaneously target cyclooxygenase-2 (COX-2) and 5-lipoxygenase (5-LOX) enzymes, effectively impeding the production of inflammatory mediators in the cyclooxygenase and lipoxygenase pathways. This dual inhibition approach enhances therapeutic efficacy while minimizing the adverse effects associated with COX-2 and 5-LOX inhibition. In this study, a comprehensive screening of 1022 molecules (analogues of compound 52) led to the identification of 18 promising COX-2/5-LOX inhibitors. The selection process involved quantitative structure-activity relationship (QSAR) analysis, utilizing 62 known inhibitors, virtual screening, molecular docking techniques, and in silico pharmacokinetic assessment. The 2D QSAR models for COX-2 and 5-LOX inhibition demonstrated high predictive accuracy (COX-2: R^2=0.9308, Q^2=0.8936; 5-LOX: R^2=0.9209, Q^2=0.8879). Docking studies further elucidated the binding affinity and specific interactions between the identified compounds and COX-2/5-LOX proteins, revealing robust hydrophobic and hydrogen bonding forces at play. ADMET analysis highlighted molecules VS864, VS865, VS882, VS888, VS895, VS896, VS897, and VS898 as optimal candidates, meeting all current drug-likeness criteria without posing any hazardous impacts. Molecular dynamic simulations confirmed the binding stabilities of the selected compounds.

Consequently, compounds VS864, VS865, VS882, VS888, VS895, VS896, VS897, and VS898 emerge as potential COX-2/5-LOX dual inhibitor candidates, paving the way for further evaluation in therapeutic applications.

Keywords: COX-2/5-LOX dual inhibitors, QSAR, virtual screening, molecular docking, pharmacokinetic analysis, Molecular Dynamic simulations

INTRODUCTION

Traditional NSAIDs are widely used for their analgesic and anti-inflammatory effects by blocking COX enzyme-associated inflammatory cytokines. Inflammation, a complex process linked to various ailments, necessitates ongoing therapy. Despite their efficacy, NSAIDs pose risks such as gastrointestinal toxicities, hepatotoxicity, and cardiovascular issues. The development of safer NSAIDs is crucial, and the COX-2/5-LOX dual inhibition strategy emerges as a promising approach **[1-5]**.

COX-2, distinct from COX-1, features a secondary pocket due to amino acid substitution, influencing selective COX-2 inhibitors. Blocking only COX-2 may shift inflammation to the LOX pathway, resulting in increased side effects. The 5-LOX enzyme, part of the liquid oxygen iso enzymes, contributes to AA metabolism and inflammatory mediator production **[6-12]**.

Compounds inhibiting both COX-2 and 5-LOX offer advantages, addressing multiple arachidonic acid pathways and exhibiting diverse anti-inflammatory properties. This dual inhibition strategy presents a potential avenue for more effective and safer drugs compared to traditional NSAIDs **[13-16]**.

Despite initial attempts with licofelone and darbufelone, a need persists for a safer COX-2/5-LOX dual inhibitor. Rational modifications, such as incorporating hydrogen bond donating groups, have been explored to enhance COX-2 selectivity. CADD, particularly QSAR, is employed in this study for lead optimization, providing insights into structural patterns governing drug activity **[17-21]**.

QSAR, a quantitative structure-activity relationship technique, aids in predicting molecular attributes' impact on activity. PaDEL-2.18 identifies descriptors, and the Genetic Algorithm module of QSARINS-V-224 optimizes descriptor selection. QSAR studies, complemented by docking, aim to create interpretable models for virtually testing novel anti-inflammatory compounds. This approach can streamline drug discovery by predicting activities and pharmacokinetic properties, saving time and resources **[22-24]**.

MATERIALS AND METHODS

QSAR Model generation

In the current investigation, a dataset consisting of 62 molecules that possessed inhibitory activity toward COX-2 and 5-

LOX was initially drawn on 2D sketcher before being converted into 3D structures with the help of the MMFF94 force field **[25–29]**. Their inhibitory activities were calculated using the pIC50 formula (pIC50=-logIC50) (IC50= Half-maximal inhibitory concentration). Because these molecules exhibit such a broad spectrum of activities (pIC50 values range from 7.678 to 3.945 for COX-2 and 6.6383 to 3.8844 for 5-LOX), the selection of these molecules for inclusion in the dataset is entirely warranted. The structures of all the molecules and their reported activity values IC50 and pIC50 are present in the supplementary materials (Appendix 1). PaDEL-Descriptor 2.18 **[30]** produced 1D, 2D, and 3D molecular descriptors and fingerprints. More than 15000 molecular descriptors describe every molecule. To avoid the inclusion of redundant and collinear molecular descriptors in the development of a robust QSAR model, QSARINS-2.2.4 was used to remove constant, nearly constant and highly correlated (correlation greater than 0.90) molecular descriptors. This reduced molecular descriptors to 69. QSARINS-2.2.4 **[19, 20]** (http://www.qsar.it) was used to forecast models with improved predictive abilities and a defined application domain. 40 compounds were used for model creation and 12 for model validation. QSARINS-2.2.4 used GA-MLR (Genetic Algorithm-Multilinear Regression) to generate optimum models. Q2 LOO was used as a fitness function to avoid overfitting and simplify the model. 10000 generations were set. According to OECD guidelines, the created models underwent internal and external statistical validation. Models with a high degree of predictability are discussed in detail.

Virtual Screening Based on QSAR model.

Using Schrodinger Software(2021-1) **[31]**, the most active compound 52 was used as a template to produce 1022 variations for QSAR-based virtual screening **(Figure 1)**. These molecules were used for QSAR based virtual screening. The three-dimensional structures of molecules were constructed in the same way as modelling sets before the molecular descriptor calculations were performed. Then, a proven QSAR model were utilised to predict new drugs' biological properties.

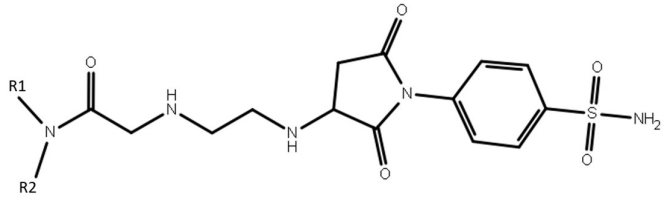

Figure 1: Compound 52 as a template for enumerations

Molecular Docking Analysis

The pdb file for cyclooxygenase- 2 receptor (PDB ID: 5KIR, resolution 2.70Å) was fetched from RCSB-PDB (https://www.rcsb.org/). Crystal structure of 5-LOX (PDB ID: 3O8Y, resolution 2.389Å) was retrieved from RCSB-PDB. The Ramachandran plot was utilised to evaluate the protein's quality **(Figure 2)**. The presence of the majority of residues in the preferred zone (shown by the red- and yellow-coloured regions) and only a few residues in the unfavourable region (represented by the white coloured region) validates the protein's suitability for docking investigations.

The simulations of molecular docking were carried out with the help of AutoDock-4.2.6, which was embedded into AutoDock Tools-1.5.6 **[32, 33]**. AutoDock tools were used to provide polar hydrogens and partial charges to the protein and ligand before the compounds were docked into the predetermined active site. Through docking of the reported drug molecules in the target protein, the location and size of the active region of the target protein, which is where substantial ligand-receptor interactions occur, were determined. A grid box of 60Å in size was constructed around the residues HIS90 and ARG513 (in the case of COX-2) **[34]** and around ILE406, TYR181, HIS600 and LEU420 (in the case of 5-LOX) **[35]**. The autodock software employs a grid-based algorithm that conducts an exhaustive search inside the binding site's dimensions. The autodock software employs a grid-based algorithm that conducts an exhaustive search inside the binding site's dimensions. The Lamarckian Genetic Algorithm (GA) was used to do research on the conformation of the ligand. The population size of the Genetic Algorithm was set to be 150, the number of GA evaluations was set to be 2500000, and the number of GA docking runs was set to 100. Each ligand was docked independently with enzymes to optimise binding. After docking, ligand binding energies at enzyme active sites were studied. By measuring the binding energies, H-bonding interactions, hydrophobic interactions, and van der Waal's interactions were examined.

a) b)

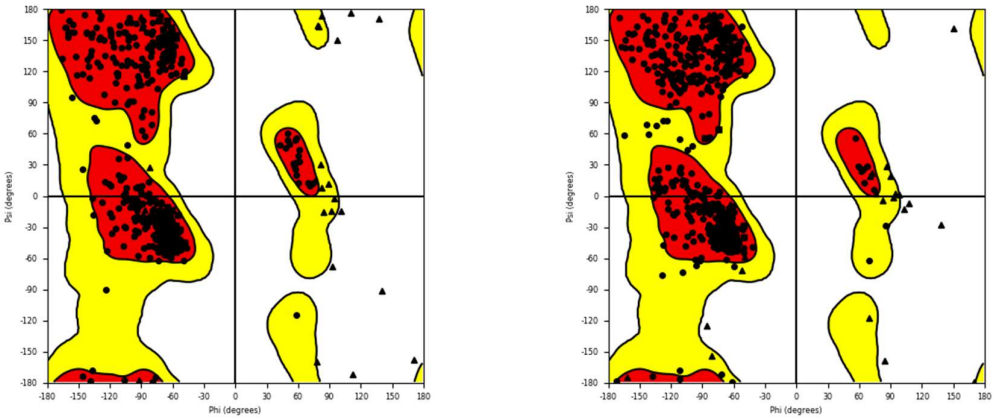

Figure 2: Ramachandran plot for a) cyclooxygenase- 2 receptor (PDB ID: 5KIR) and b) 5-lipoxygenese (PDB ID: 3O8Y)

Pharmacokinetic property study

All 18 virtually screened compounds' pharmacokinetic characteristics (ADMET) were evaluated using ADMETLab 2.0 **[36]**, which has a stronger capacity to aid medicinal chemists in quickening the drug research and development process. For the pharmacokinetic property prediction, each compound's SMILES notation was employed.

Molecular Dynamic Simulations

All the MD simulations were done using the NAMD package (Version 2.14) developed by the Theoretical and Computational Biophysics Group in the Beckman Institute for Advanced Science and Technology at the University of Illinois at Urbana−Champaign with the CHARMM 36 force field **[37]**. The dynamic simulations were done using TIP3P water box with a padding of 5Å keeping temperature and pressure constant at 310 K and 1 atm respectively for 20ns. The preparation and analysis were carried out using VMD package 1.9.3 (available at **http://www.ks.uiuc.edu/Research/vmd/**) **[38]**.

RESULT AND DISCUSSIONS

QSAR model generation and its validation

QSAR is a valuable method for predicting molecular activity based on structural features. QSAR models correlate chemical descriptors with structural characteristics, emphasizing goodness of fit, robustness, and predictability. Adhering to OECD criteria ensures reliability and reproducibility. Evaluating 62 structurally similar compounds with specified COX-2 and 5-LOX inhibition using the same bioassay approach, QSAR models were generated. QSARINS employed a multiple linear regression (MLR) analysis with a genetic algorithm (GA) set to 5 descriptors, producing statistically meaningful models.

The following are the best GA-MLR models for COX-2 and 5-LOX:

GA-MLR QSAR Model for COX2 inhibitors

$$pIC50 = 1.0702(\pm 0.7660) + 0.2941(\pm 0.2678) * C1SP2 - 7.0059(\pm 2.5870) * MDEN12 + 0.6293(\pm 0.4786) * MLFER_A + 0.6567(\pm 0.1459) * nTRing + 0.3248(\pm 0.08) * nRotB$$

GA-MLR QSAR Model for 5-LOX inhibitors

$$pIC50 = 2.7443(\pm 0.3839) + 0.2358(\pm 0.0438) * nBondsD + 0.2572(\pm 0.1439) * C3SP2 + 0.7215(\pm 0.1153) * n6HeteroRing - 0.5564(\pm 0.3232) * PubchemFP192 + 0.3419(\pm 0.1945) * PubchemFP300$$

The performance of 2D QSAR model developed for COX-2 and 5-LOX were presented in **Table 1**.

Table 1: Performance of 2D QSAR model developed by QSARINS for COX-2 and 5-LOX inhibitors.

Validation parameters	COX-2	5-LOX	Validation parameters	COX-2	5-LOX
R^2	0.9308	0.9209	CCC cv	0.9452	0.9418
R^2adj	0.9206	0.9068	Q2 LMO	0.8772	0.8791
LOF	0.13	0.1034	R2 Yscr	0.1255	0.1544
RMSE tr	0.2705	0.227	Q2 Yscr	-0.2462	-0.2564
MAE tr	0.2076	0.1816	RMSE ext	0.4648	0.2946
CCC tr	0.9641	0.9588	MAE ext	0.3066	0.181
s	0.2933	0.2502	R2ext	0.779	0.8575
F	91.4116	65.214	Q2-F1	0.7722	0.8492
Q^2loo	0.8936	0.8879	Q2-F2	0.7326	0.8461
RMSE cv	0.3352	0.2703	Q2-F3	0.7955	0.8668
MAE cv	0.2537	0.2187	CCC ext	0.8781	0.9254

Figures 3 and 4 illustrate the experimental versus projected pIC50 values for COX-2 and 5-LOX GA-MLR models, respectively, along with Williams plots assessing the application domain of each model. Multiple QSAR models meet threshold values for statistical parameters, indicating their reliability. Close alignment of R^2, R_{adj}^2, LOF, and R_{cv}^2 values suggests an optimal number of variables without overfitting. The high Q_{LMO}^2 value confirms satisfactory internal validation, while low R_{Yscr}^2 and Q_{Yscr}^2 values indicate the absence of random correlations. Elevated R_{ex}^2, Q^2-Fn, and CCC_{ext} values demonstrate adequate external predictive capacity, and F-ratio values signify statistical significance.

For COX-2 inhibitory activity, independent variables include C1SP2, MDEN-12, MLFER_A, nTRing, and nRotB, with positive coefficients indicating increased projected activity and negative coefficients implying a decline.

5-LOX inhibitory activity depends on nBondsD, C3SP2, n6HeteroRing, PubchemFP192, and PubchemFP300, highlighting their influence on activity.

Virtual Screening Based on QSAR model

Molecules having an anticipated COX-2 inhibitory activity that was larger than 7.50 were chosen for the prediction of their 5-LOX inhibitory activity, docking analysis, and pharmacokinetic property investigations. This resulted in the selection of 18 different molecules. The 18 most active compounds, as predicted by the generated QSAR models (COX-2 and 5-LOX), are shown in the **Figure 5**. According to the model, increasing the independent variables (except *MDEN-12* for which a decrease in the value will result in increased pIC50 value) proposed by the QSAR model equation for COX-2 inhibition could result in a higher pIC50 value for a molecule.

a) b)

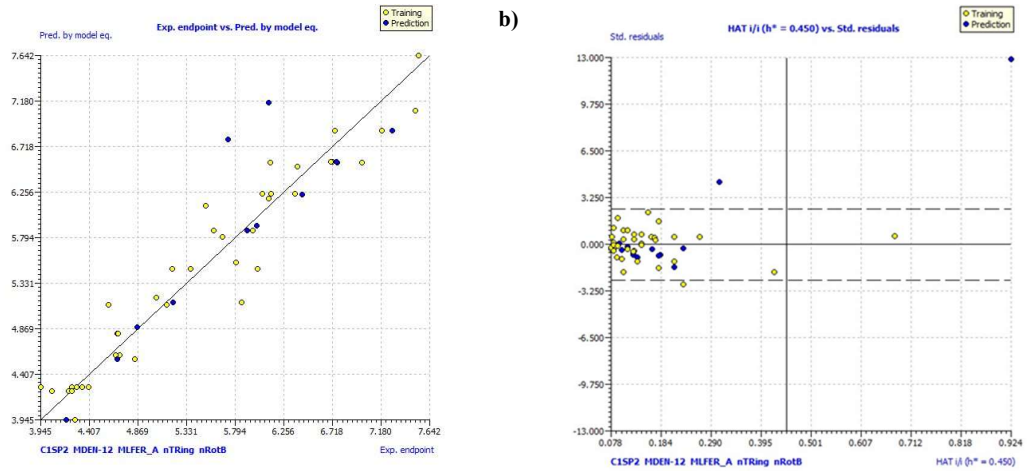

Figures 3: a) The experimental versus projected pIC50 values for the COX-2 GA-MLR model and b) Williams plot to examine the application domain of the model

a) b)

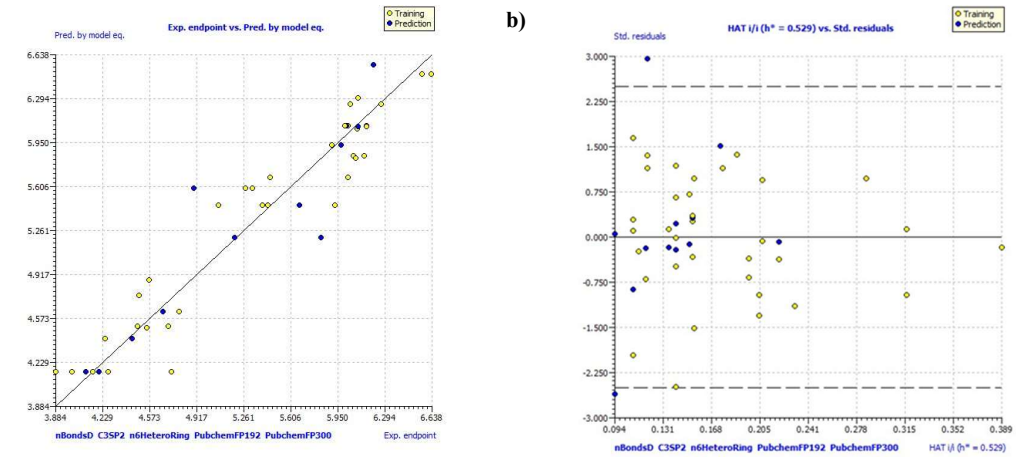

Figure 4: a) The experimental versus projected pIC50 values for 5-LOX GA-MLR model and b) Williams the two models to examine the application domain of the model.

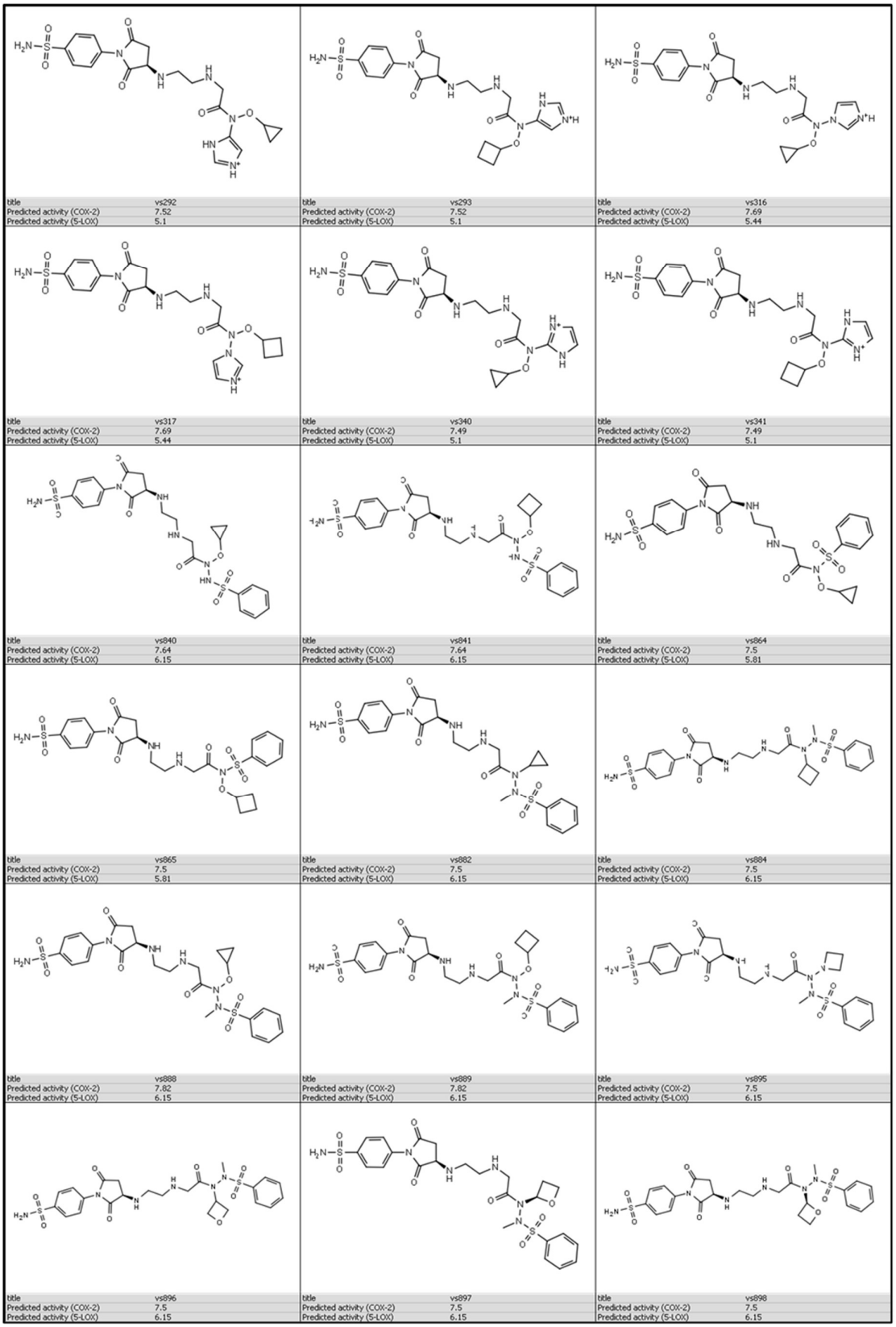

Figure 5: Structures and predicted pIC50 values (COX-2 and 5-LOX) of 18 virtually screened molecules

Molecular Docking Analysis

Molecular docking, a crucial structure-based drug development approach in computer-assisted drug design (CADD), predicts bioactive conformations of molecules by identifying key interacting residues, binding interactions, and scoring functions. Celecoxib, an approved COX-2 inhibitor (pIC50 = 7.30), served as a reference drug for docking to elucidate essential properties for efficient COX-2 inhibition. **Figure 6** displays 2D and 3D ligand interaction diagrams.

Eighteen molecules, selected based on a pIC50 value greater than 7.50 from virtual screening using the COX-2 QSAR model, underwent molecular docking against the grid derived from the reference molecule's docking. Docking scores and interacting residues of celecoxib and the 18 molecules are summarized in **Table 2**, with VS865 and VS896 exemplifying docking postures **(Figure 7)**. Their docking scores are -9.76 kcal/mol and -9.66 kcal/mol, respectively.

Celecoxib establishes hydrogen bonding with SER353, ILE517, HIS90, GLN192, PHE518, and LEU352, engages in amide-pi stacking hydrophobic interactions with LEU352, and forms alkyl or pi-alkyl hydrophobic interactions with LEU359, MET522, ALA527, TRP387, VAL523, VAL349, and PHE518. These interactions enhance the stability of celecoxib binding to the COX-2 active site, resulting in a lower free energy of binding (-10.78 kcal/mol).

While docking 18 virtually screened molecule, it was observed that except VS316 and VS340, the $-S=O$ oxygen of all other compounds form hydrogen bonding interactions with PHE518. The residues SER353, ILE517, GLN192, and LEU352 are also important contributors to the formation of hydrogen bonding connections with $-SO_2-NH_2$ group of ligand molecules. Excluding VS292, VS293, VS316, VS340, VS884, and VS895, the remaining 12 molecules formed hydrogen bonding interactions with ARG120. All compounds exhibited alkyl/pi-alkyl hydrophobic interactions with VAL523, LEU93, and VAL89 as crucial residues. VS316 and VS340 additionally demonstrated pi-sulphur interactions with TRP387. Pi-cation interactions were observed between ARG120 and the pi-electron cloud of phenyl rings in VS840, VS896, and VS889, with estimated free binding energies of -9.13 and -9.76 kcal/mol, respectively. For VS864 and VS896, the pi-electron cloud of the amide linkage in LEU352 created a hydrophobic connection with the pi-electron cloud of benzene rings in the ligands. LEU352 and SER353 participated in pi-sigma hydrophobic interactions with VS864 and VS889, respectively.

Molecular docking with the 5-LOX protein, using Zileuton as the reference, employed active site residues ILE406, PHE177, TYR181, THR364, ASN407, LEU420, PHE421, HIS432, TRP599, HIS600, ALA603, and ALA606 to construct a grid. Docking scores and interaction residues for Zileuton and high-binding-energy molecules (VS882, VS864, VS865, VS896, and VS898) are presented in **Table 3**. Hydrogen bonding and hydrophobic interactions were identified as responsible for the high negative binding energies, with most compounds engaging LEU368, ALA603, ALA410, TYR181, TRP599, PHE421, ILE415, and HIS367. **Figure 9** illustrates 2D interaction graphs for Zileuton and VS865 with the 5-LOX protein.

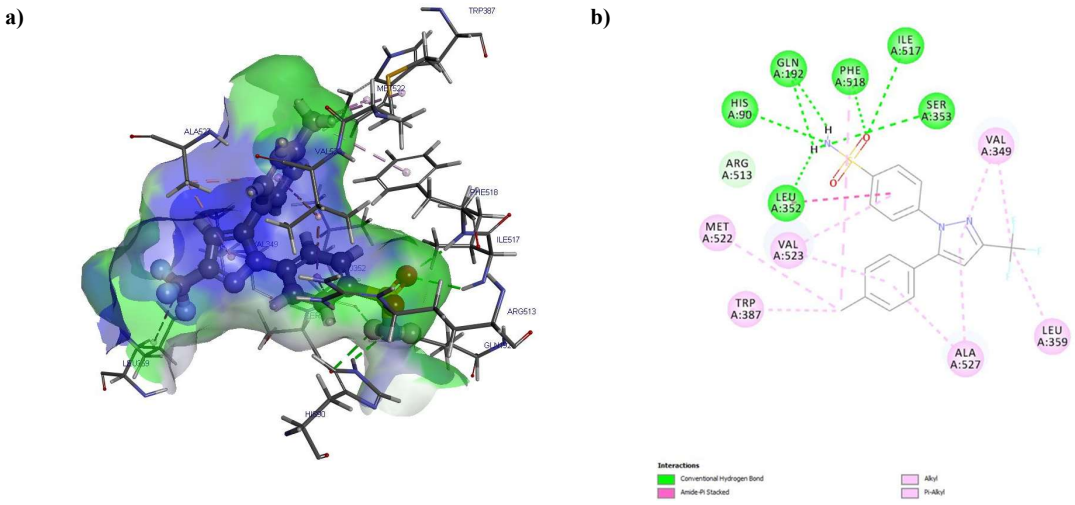

Figure 6: a)3D and b) 2D ligand interaction diagrams of Celecoxib with COX-2

Pharmacokinetic property predictions

The 18 compounds underwent pharmacokinetic property prediction using ADMETLab 2.0. **Table 4** summarizes their physicochemical qualities and medicinal properties, along with the required ideal limits for drug-like behavior. Each molecule exhibits desirable drug-like characteristics, with over 12 hydrogen bond acceptors. Specifically, molecules VS316, VS317, VS840, and VS841 possess 7 hydrogen bond donor sites, while VS292, VS293, VS340, and VS341 have 8. The formal charge for each molecule is either 0 or 1. Notably, the topological polar surface area (TPSA), representing the total surface contributions of polar segments, exceeded 140 for all 18 molecules. TPSA is crucial for

drug absorption, and its values in our compounds suggest potential efficacy.

Moreover, the anticipated solubility (logS) of these compounds falls within the acceptable range of -4 to 5 logmol/L. Adequate solubility is crucial for optimal drug absorption, ensuring effective dissolution and absorption in the gastrointestinal tract.

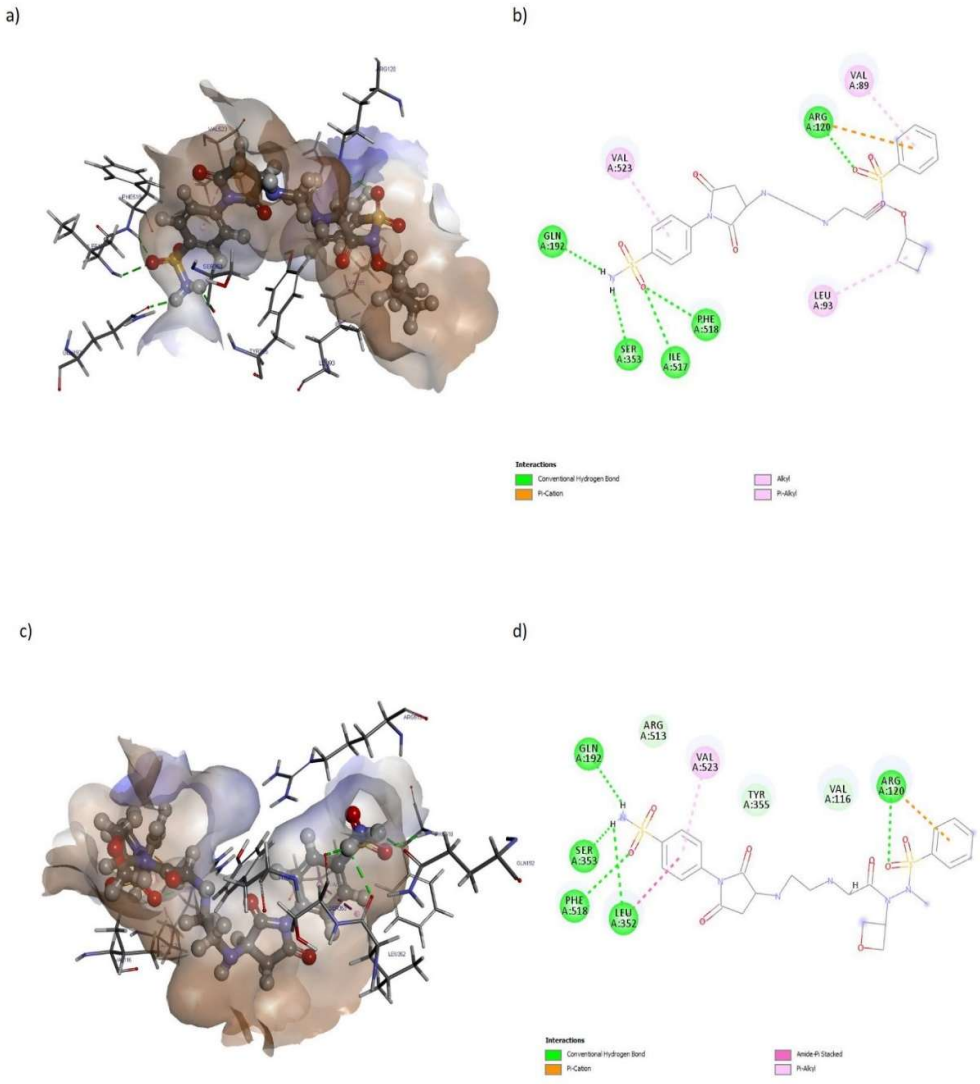

Figure 7: Docking pictures of ligands with COX-2 protein. a) 3D conformation of VS865 b) 2D interaction diagram of VS865 c) 3D conformation of VS896 and d) 2D interaction diagram of VS 896

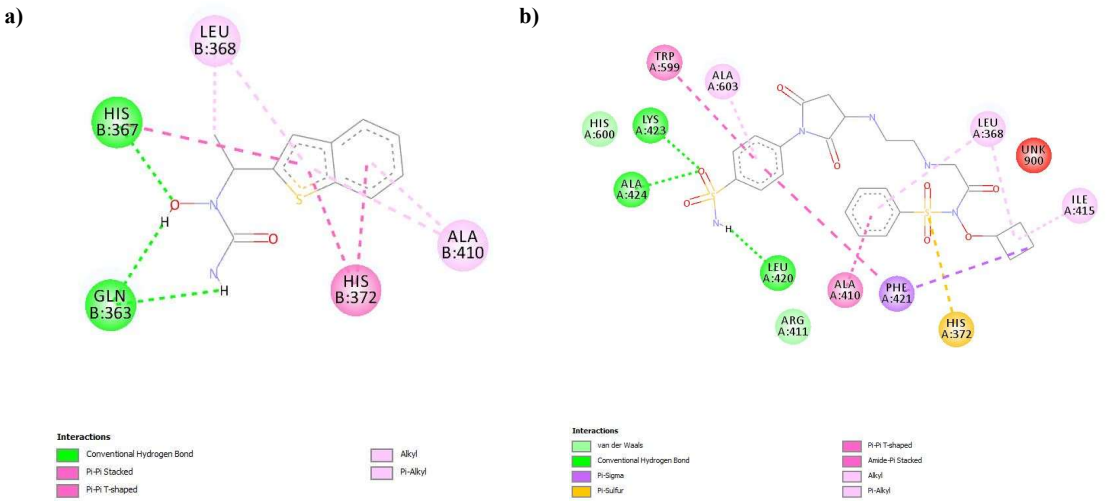

Figure 8: 2D interaction graphs of a) Zileuton and b) VS865 with 5-LOX protein

Table 2: The docking score and the interacting residues of celecoxib and 18 molecules

Compound	Predicted pIC50	Docking score (kcal/mol)	Interacting residues
Celecoxib	*7.4	-10.78	SER 353, LEU352, HIS90, GLN192, ILE517, PHE518, TYR355, VAL349, ALA527, VAL523
VS292	7.52	-8.27	PHE518, LEU352, GLN192, TYR385, TRP387, VAL523
VS292	7.52	-8.81	PHE518, ILE517, SER353, LEU352, GLN192, TYR355, PRO86, VAL523, VAL89, ARG513
VS316	7.68	-8.53	TYR385, SER530, LEU352, ASP515, GLN192, LEU352, TRP387, HIS356
VS317	7.68	-8.52	ARG120, PHE518, ILE517, LEU352, HIS90, GLN192, VAL89, VAL523
VS340	7.5	-7.47	TYR385, SER530, SER353, TRP387, HIS95, GLY526, ALA527, VAL523, LEU352, HIS356, PRO514
VS341	7.5	-9.5	GLN192, SER353, ILE517, PHE518, ARG120, SER530, SER353, TYR385, VAL523, TRP387, TYR385
VS840	7.64	-9.13	ARG120, TYR355, PHE518, ILE517, SER353, LEU352, GLN192, LEU93, VAL523
VS841	7.64	-9.34	PHE518, GLN192, LEU352, HIS90, TYR355, ARG120, VAL89, LEU93, VAL523
VS864	7.5	-9.36	LEU352, GLN192, SER353, PHE518, ARG120, VAL89, LEU352, LEU93, VAL523
VS865	7.5	-9.76	ILE517, PHE518, SER353, GLN192, ARG120, VAL523, VAL89, LEU93
VS882	7.5	-8.52	ARG120, ILE517, PHE518, HIS90, ARG120, VAL89, LEU93, VAL323
VS884	7.5	-8.73	LEU352, SER353, ILE517, PHE518, GLN192, TYR115, LEU352, LEU93, VAL116, VAL523

VS888	**7.82**	**-8.24**	**ARG120, ALA527, LEU93, VAL116, VAL523, ALA516, PHE518**
VS889	**7.82**	**-9.29**	**ARG120, HIS90, GLN192, LEU352, PHE518, ILE517, SER353, VAL89, LEU93, VAL523**
VS895	**7.5**	**-8.98**	**PHE518, SER353, LEU352, GLN192, TYR348, LEU352, LEU534, MET522, TRP387, PHE518, VAL523**
VS896	**7.5**	**-9.66**	**GLN192, SER353, PHE518, LEU352, ARG120, VAL523**
VS897	**7.5**	**-8.39**	**GLN192, PHE518, ILE517, ARG120, TYR115, LEU93, VAL89, VAL523**
VS898	**7.5**	**-9.27**	**ILE517, SER353, LEU352, PHE518, GLN192, ARG120, LEU93, VAL89, VAL523**

*** Estimated value**

Table 3: The docking score and the interacting residues of zileuton and VS882, VS864, VS865, VS896, and VS898

Compound	Predicted pIC50	Docking score (kcal/mol)	Interacting residues	Interactions
Zileuton	***6.20**	**-8.74**	**HIS 367, GLN363, HIS372, ALA410, LEU368**	**Hydrogen bonding, alkyl/ pi-alkyl hydrophobic interactions, pi-pi T shaped interactions**
VS864	**5.81**	**-8.64**	**ASN425, ALA424, TRP599, HIS372, TYR181, LEU368, ILE415, ALA410, ARG411, ALA603**	**Hydrogen bonding, alkyl/ pi-alkyl hydrophobic interactions, T shaped pi-pi hydrophobic interactions, Pi-lone pair interactions**
VS865	**5.81**	**-8.86**	**LYS423, ALA424, LEU420, PHE421, TRP599, ALA410, LEU368, ILE415, ALA603**	**Hydrogen bonding, alkyl/ pi-alkyl hydrophobic interactions, amide-pi stacked / T shaped pi-pi hydrophobic interactions**
VS882	**6.15**	**-7.92**	**GLU376, GLN363, ALA410, PHE359, HIS367, ALA603, LEU368, TYR181**	**Hydrogen bonding, alkyl/ pi-alkyl hydrophobic interactions, pi-sigma interactions, amide-pi stacked / T shaped pi-pi hydrophobic interactions**
VS896	**6.15**	**-8.38**	**HIS367, ASN425, LYS423, ALA424, PHE421, TYR181, LEU368, ILE415, ALA603, HIS372**	**Hydrogen bonding, alkyl/ pi-alkyl hydrophobic interactions, pi-pi interactions, pi-sigma interactions**
VS898	**6.15**	**-8.58**	**LEU368, GLN557, GLN363, TRP599, PHE421, PHE177, ALA140, ILE406, PHE421, ALA603**	**Hydrogen bonding, alkyl/ pi-alkyl hydrophobic interactions, Pi-sulphur interactions, pi-pi T shaped interactions**

*** Estimated value**

A medicine must enter the bloodstream and reach its target to be therapeutic. To dissolve in bodily fluid and permeate biomembranes, consumable medications must balance lipophilicity and hydrophilicity. In the early stages of drug discovery, it is necessary to measure n-octanol/water distribution coefficients at physiological pH (logD7.4) Except for VS292 and VS316 (LogD7.4: -0.294 and -0.06mol/L), all other compounds exhibited suitable values. The outputs of the desirability functions based on the molecular weight (MW), the logP, the number of hydrogen bond acceptors (nHA), the number of hydrogen bond donors (nHD),

TPSA, the number of rotatable bonds, the number of aromatic rings, and the number of alerts for undesirable functional groups are integrated to produce QED **[39]**. These molecules were the least suitable as drugs since their QED was less than 0.67 in all the compounds studied. According to the Lipinski rule, a drug-like molecule must meet the following criteria: MW≤500; LogP≤5; nHA≤10; and nHD≤5. Poor absorption or permeability can occur when two characteristics are out of range. In this case, none of the compounds studied followed the Lipinski rule **[40]**. However, all compounds met the Pfizer criteria **[41]**, which states that logP>3; TPSA<75 are likely to be harmful. All of the molecules in this area were inside the parameters. One of the most well-known common fitters is Pan Assay interference compounds (PAINS) **[42]**, which consists of 480 substructures produced from the study of FHs determined by six target-based HTS assays. It is easy to screen false positive findings and identify problematic substances in screening databases using these filters. Because all 18 compounds have a PAINS score of zero, this implies that they are safe. Since all of the compounds have a synthetic accessibility score (SAscore) **[43]** of less than six, this suggests that it is not difficult to produce any of the molecules. **Table 5** displays the anticipated absorption and distribution property scores for the 18 virtually screened compounds by ADMETLab2.0. For oral medications, passage through intestinal cell membranes is crucial, involving passive diffusion, carrier-mediated absorption, or active transport. Human colon adenocarcinoma cell lines (Caco2) are often used to assess in vivo drug permeability, with a benchmark score of -5.15log cm/s. However, all 18 compounds exhibit scores below this threshold, suggesting potential limitations as drug candidates.

Table 4: Physicochemical properties of 18 virtually screened compounds

Compound	MW*	nHA*	nHD*	TPSA*	nRot*	fChar*	LogS	LogD7.4	LogP	QED	SA score*	Lipinski	Pfizer
Desirable limits	100-600	0-12	0-7	0-140	0-11	-4 to 4	-4 to 0.5 logmol/L	1 - 3 logmol/L	0 - 3 logmol/L	>0.67: excellent	≤6: excellent	MW≤500; LogP≤5; nHA≤10; nHD≤5	logP>3; TPSA<75
VS292	492.17	13	8	189.08	12	1	-3.228	-0.294	-0.721	0.157	3.978	Rejected	Accepted
VS293	506.18	13	8	189.08	12	1	-3.334	0.026	-0.391	0.157	3.955	Rejected	Accepted
VS316	492.17	13	7	178.22	12	1	-3.001	-0.06	-0.432	0.174	4.004	Rejected	Accepted
VS317	506.18	13	7	178.22	12	1	-3.079	0.221	-0.082	0.175	3.98	Rejected	Accepted
VS340	492.17	13	8	189.08	12	1	-2.964	0.232	-0.703	0.157	3.947	Rejected	Accepted
VS341	506.18	13	8	189.08	12	1	-3.075	0.601	-0.301	0.157	3.925	Rejected	Accepted
VS840	580.14	14	7	205.32	14	0	-3.581	0.659	0.202	0.121	3.314	Rejected	Accepted
VS841	594.16	14	7	205.32	14	0	-3.693	1.014	0.393	0.121	3.321	Rejected	Accepted
VS864	565.13	13	6	193.29	13	0	-3.66	0.18	0.379	0.155	3.195	Rejected	Accepted
VS865	579.15	13	6	193.29	13	0	-3.773	0.506	0.677	0.154	3.203	Rejected	Accepted
VS882	578.16	13	6	187.3	13	0	-3.616	0.253	0.391	0.153	3.219	Rejected	Accepted
VS884	592.18	13	6	187.3	13	0	-3.713	0.567	0.645	0.152	3.233	Rejected	Accepted
VS888	594.16	14	6	196.53	14	0	-3.571	0.73	0.419	0.139	3.371	Rejected	Accepted
VS889	608.17	14	6	196.53	14	0	-3.695	1.078	0.697	0.138	3.378	Rejected	Accepted
VS895	593.17	14	6	190.54	13	0	-3.035	0.126	0.229	0.143	3.304	Rejected	Accepted
VS896	594.16	14	6	196.53	13	0	-3.508	0.104	0.019	0.141	3.328	Rejected	Accepted
VS897	594.16	14	6	196.53	13	0	-3.384	0.28	0.22	0.144	3.768	Rejected	Accepted
VS898	594.16	14	6	196.53	13	0	-3.384	0.28	0.22	0.144	3.768	Rejected	Accepted

*MW- Molecular weight; nHA- number of Hydrogen bond acceptors; nHD- number of Hydrogen bond donors, TPSA- Topological polar surface area; nRot- number of rotatable bonds; fChar-formal charge; SA score- Synthetic accessibility score

MDCK cells (Madin-Darby Canine Kidney Cells) serve as an in vitro permeability model, and their apparent permeability coefficient (Papp) is a gold standard for assessing chemical effectiveness in the body in vitro. Blood-Brain Barrier (BBB) influence is estimated using Papp values from MDCK cell lines. In this study, except for VS292, VS293, VS316, VS317, VS340, and VS341, all other compounds show notable MDCK permeability values, indicating high passive MDCK permeability when Papp exceeds 2×10^{-6} cm/s.

Table 5: The anticipated absorption and distribution property scores of 18 virtually screened compounds

Compound	Caco-2	MDCK	HIA	F(20%)	BBB	PPB
Desirable limits	>5.15: excellent	>2E-06: excellent	0-0.3: excellent 0.3-0.7:medium 0.7-1.0 poor	0-0.3: excellent 0.3-0.7:medium 0.7-1.0 poor	0-0.3: excellent 0.3-0.7:medium 0.7-1.0 poor	≤90%: excellent
VS292	-6.038	1.33E-06	0.948	0.961	0.147	33.52%
VS293	-6.002	1.27E-06	0.937	0.97	0.155	29.55%
VS316	-6.159	1.32E-06	0.961	0.881	0.396	47.03%
VS317	-6.107	1.26E-06	0.95	0.911	0.381	44.89%
VS340	-6.058	1.35E-06	0.923	0.626	0.186	28.61%
VS341	-5.994	1.34E-06	0.913	0.707	0.183	25.14%
VS840	-6.763	4.74E-06	0.843	0.258	0.006	62.99%
VS841	-6.678	4.86E-06	0.831	0.193	0.005	64.88%
VS864	-6.285	4.36E-06	0.241	0.931	0.094	71.72%
VS865	-6.209	4.53E-06	0.163	0.931	0.074	74.60%
VS882	-6.824	3.67E-06	0.011	0.014	0.114	64.63%
VS884	-6.759	3.85E-06	0.012	0.018	0.085	67.23%
VS888	-6.621	4.34E-06	0.038	0.042	0.05	64.59%
VS889	-6.542	4.4E-06	0.035	0.042	0.043	66.27%
VS895	-6.686	2.39E-06	0.024	0.335	0.035	67.84%
VS896	-6.785	4.26E-06	0.012	0.233	0.105	64.76%
VS897	-6.78	4.36E-06	0.032	0.022	0.079	64.47%
VS898	-6.78	4.36E-06	0.032	0.022	0.079	64.47%

Table 6: The findings of 18 virtually screened substances' anticipated metabolic properties and $T_{1/2}$.

Compound	CYP1A2-inh	CYP2C19-inh	CYP2C9-inh	CYP2D6-inh	CYP3A4-inh	$T_{1/2}$
Desirable limits	0 to 1	0 to 1	0 to 1	0 to 1	0 to 1	≤ 3
VS292	0.013	0.031	0.03	0.092	0.034	0.927
VS293	0.015	0.034	0.041	0.131	0.045	0.927
VS316	0.035	0.117	0.111	0.472	0.026	0.923
VS317	0.042	0.134	0.175	0.573	0.037	0.924
VS340	0.002	0.028	0.01	0.005	0.013	0.82
VS341	0.003	0.029	0.011	0.008	0.018	0.797
VS840	0.008	0.024	0.068	0.012	0.062	0.194
VS841	0.011	0.027	0.118	0.018	0.114	0.186
VS864	0.017	0.026	0.338	0.022	0.141	0.272
VS865	0.021	0.029	0.483	0.044	0.249	0.252
VS882	0.004	0.022	0.121	0.002	0.232	0.202
VS884	0.004	0.024	0.178	0.004	0.449	0.178
VS888	0.009	0.026	0.212	0.002	0.14	0.226
VS889	0.011	0.029	0.299	0.004	0.261	0.202
VS895	0.004	0.018	0.037	0	0.126	0.207
VS896	0.002	0.016	0.069	0.001	0.095	0.288
VS897	0.003	0.018	0.072	0.001	0.08	0.323
VS898	0.003	0.018	0.072	0.001	0.08	0.323

Table 5 presents ADMETLab2.0's anticipated absorption and distribution property scores for the 18 compounds. Human Intestinal Absorption (HIA) values above 30% are considered suitable for oral bioavailability. VS864, VS865, VS882, VS884, VS888, VS889, VS895, VS896, VS897, and VS898 meet this criterion, making them potential drug candidates. Human oral bioavailability, a crucial pharmacokinetic criterion, designates molecules with F20% (the human oral bioavailability 20%) as having good oral bioavailability. VS840, VS841, VS882, VS884, VS888, VS889, VS895, VS896, VS897, and VS898 were identified as orally bioavailable. Plasma protein binding (PPB) is significant for drug delivery, influencing oral bioavailability. All 18 compounds have anticipated PPB values above 90%, indicating valid PPB. Blood-Brain Barrier (BBB) penetration is essential for drugs targeting the CNS, while some drugs may require minimal or no BBB penetration for peripheral targets. VS316 and VS317 show a medium BBB penetration probability, and all other compounds have a BBB+ possibility. Drug metabolism, assessed through metabolic activity scores, falls within the ideal range for all compounds. **Table 6** details the predicted results. Except for VS292, VS293, VS316, VS317, VS340, and VS341, all compounds have $T_{1/2} \leq 3$, representing a composite term for a drug's half-life involving clearance and distribution volume. Cardiotoxicity, evaluated through hERG inhibition, shows VS316 and VS317 as highly active, while others exhibit moderate activity. Hepatotoxicity predictions suggest potential harm for all molecules. Mutagenicity and carcinogenicity assessments indicate that VS293, VS897, and VS898 are non-carcinogenic, whereas VS340, VS341, VS864, VS865, VS882, VS884, and VS896 have a medium carcinogenic potential. Respiratory toxicity predictions show non-respiratory toxicants for VS316, VS317, VS864, VS865, VS882, VS884, VS895, VS896, VS897, and VS898, while VS292, VS293, VS340, and VS341 fall within a medium respiratory toxicity range. Endocrine disruption evaluations reveal no disruptions in androgen-estrogen balance (output values 0-0.3). Estrogen receptor interactions also indicate no impact on normal endocrine function. Oxidative stress evaluations suggest medium to active activity for all compounds in the ARE signalling pathway, indicating potential safety. Tumour suppressor protein p53 activation is observed for all compounds, and Heat Shock Response (HSR) activation is likely for all molecules. Toxicological study results are summarized in **Table 7**. The pharmacokinetic study indicates compliance with the Pfizer rule for all molecules. VS864, VS865, VS882, VS884,

VS895, VS896, VS897, and VS898 are identified as less hazardous with drug-like properties, suggesting their potential as therapeutic molecules.

Molecular Dynamics Simulations

Since the protein is highly flexible conformational changes occurs will ligand binding which cannot be anticipated highly by molecular docking analysis. RMSD (Root Mean square deviation) analysis by molecular dynamics simulations aids in the estimation of repositioning of protein backbone upon formation of the docked complexes **[44]**. Eight hit compounds were subjected to MD analysis and RMSD values were compared with that of apoprotein. The protein and the ligands VS864, VS865, VS882, VS884, VS895, VS896, VS897, VS898 yielded average RMSDs of 2.09, 1.69, 1.91, 1.69, 1.69, 1.89, 1.16, 1.69 and 1.91 Å respectively. The RMSD plot is given in figure 10. Inspecting the figure, all the ligands reached a plateau after 17 ns. All the ligands have furnished RMSDs less than the apoprotein leading to stable docked complexes.

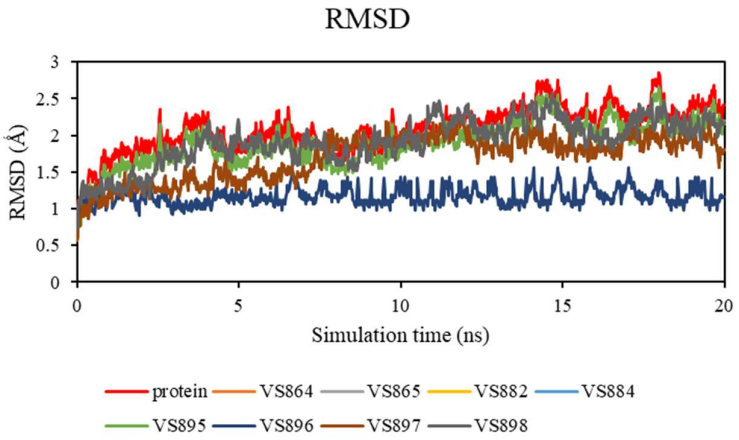

Figure 9: RMSD plot protein and docked complexes

CONCLUSION

Recent advancements in computational processes have revolutionized drug discovery, overcoming the challenges associated with the traditional complex, expensive, and time-consuming methods. Both structure-based and ligand-based virtual screening approaches offer efficient means to identify hits and optimize leads for clinical drug development programs. This study focuses on the development of COX-2/5-LOX dual inhibitors, targeting prostaglandins and leukotrienes—critical inflammatory mediators. Utilizing in silico methods, our objective was to identify potential COX-2/5-LOX dual inhibitors from a vast dataset of 1022 compounds. We initiated the study with 2D QSAR

experiments on 62 COX-2/5-LOX inhibitor compounds, aiming to establish a robust model for the screening of potent molecules as COX-2 and 5-LOX dual inhibitors. Through comprehensive statistical analyses involving fingerprints, as well as 2D and 3D molecular descriptors, we successfully developed reliable QSAR models for COX-2 inhibition and 5-LOX inhibition. As a result, highly predictive models were created, each of which exhibited a high degree of correlation with the training set as well as the test set ($R^2 = 0.9308$ and $Q^2 = 0.8936$ for COX-2 inhibition and $R^2 = 0.9209$ and $Q^2 = 0.8879$ for 5-LOX inhibition). The cross validated R^2 value and Y scrambling values were used to determine the models' effectiveness. Using the developed QSAR models, we screened 1022 derivatives of compound 52, which had the highest experimentally determined pIC50 value for COX-2 inhibition. Out of the total molecules, 18 compounds were identified with predicted pIC50 values exceeding 7.5. Subsequently, docking studies were conducted with celecoxib as a reference, revealing that hydrophobic contacts and hydrogen bonding connections enhance inhibitory activity. The active compounds for COX-2 inhibition demonstrated prevalent hydrophobic interactions with LEU93, VAL89, VAL349, and LEU352, along with hydrogen bonding interactions involving PHE518, GLN192, SER353, ILE517, LEU352, and ARG120. In the case of 5-LOX inhibition, active compounds exhibited frequent hydrogen bonding interactions with GLN363 and hydrophobic interactions with LEU368, ALA603, and ALA410. All 18 compounds showing significant interactions with the target protein were subjected to pharmacokinetic investigations. Following current drug-likeness recommendations, the pharmacokinetic features, along with the ADMET study, highlight that VS864, VS865, VS882, VS884, VS895, VS896, VS897, and VS898 are potential candidates as they lack potentially harmful effects. Molecular dynamics investigations were employed to assess binding stability and conformational changes in the protein-ligand complexes of these top eight compounds. Consequently, these compounds present themselves as promising candidates in the development of potent COX-2/5-LOX dual inhibitors.

Acknowledgements

The authors would like to thank University of Kerala for comprehending this research work. We owe a special thanks to Dr. A Muhammed Thaha, Principal, Milad-E-Sherief Memorial College in Kayamkulam, who has been supportive of our professional objectives and has worked hard to ensure that we have the protected academic time we need to pursue them.

Table 7: Toxicological study results

Compound	hERG	H-HT	AMES	Carcinogenicity	Respiratory	NR-Aromatase	NR-ER	SR-ARE	SR-ATAD5	SR-HSE	SR-p53
Desired limits	0-0.3: excellent 0.3-0.7: medium 0.7-1.0: poor	0-0.3: excellent 0.3-0.7: medium 0.7-1.0: poor	0-0.3: excellent 0.3-0.7: medium 0.7-1.0: poor	0-0.3: excellent 0.3-0.7: medium 0.7-1.0: poor	0-0.3: excellent 0.3-0.7: medium 0.7-1.0: poor	0-0.3: excellent 0.3-0.7: medium 0.7-1.0: poor	0-0.3: excellent 0.3-0.7: medium 0.7-1.0: poor	0-0.3: excellent 0.3-0.7: medium 0.7-1.0: poor	0-0.3: excellent 0.3-0.7: medium 0.7-1.0: poor	0-0.3: excellent 0.3-0.7: medium 0.7-1.0: poor	0-0.3: excellent 0.3-0.7: medium 0.7-1.0: poor
VS292	0.386	0.652	0.707	0.019	0.444	0.194	0.065	0.543	0.008	0.005	0.37
VS293	0.398	0.672	0.701	0.02	0.487	0.278	0.066	0.595	0.008	0.007	0.393
VS316	0.23	0.752	0.996	0.884	0.231	0.012	0.081	0.223	0.004	0.001	0.029
VS317	0.242	0.759	0.996	0.879	0.238	0.017	0.082	0.249	0.004	0.001	0.029
VS340	0.609	0.809	0.635	0.435	0.52	0.02	0.164	0.587	0.009	0.004	0.369
VS341	0.62	0.818	0.621	0.462	0.552	0.028	0.171	0.64	0.009	0.005	0.391
VS840	0.426	0.952	0.987	0.933	0.855	0.01	0.276	0.649	0.005	0.003	0.122
VS841	0.439	0.953	0.986	0.932	0.856	0.013	0.283	0.685	0.005	0.004	0.13
VS864	0.407	0.897	0.024	0.519	0.042	0.012	0.209	0.382	0.003	0.001	0.023
VS865	0.42	0.898	0.024	0.507	0.045	0.015	0.214	0.416	0.003	0.001	0.025
VS882	0.668	0.979	0.017	0.344	0.241	0.004	0.118	0.51	0.003	0.002	0.005
VS884	0.665	0.977	0.017	0.302	0.267	0.005	0.121	0.543	0.003	0.002	0.005
VS888	0.446	0.964	0.968	0.902	0.813	0.021	0.17	0.539	0.004	0.003	0.038
VS889	0.462	0.965	0.966	0.895	0.817	0.025	0.174	0.579	0.004	0.003	0.041
VS895	0.582	0.99	0.239	0.914	0.803	0.002	0.08	0.209	0.003	0.001	0.002
VS896	0.526	0.961	0.022	0.527	0.074	0.006	0.121	0.375	0.003	0.002	0.006
VS897	0.543	0.973	0.016	0.209	0.093	0.006	0.14	0.498	0.004	0.002	0.007
VS898	0.543	0.973	0.016	0.209	0.093	0.006	0.14	0.498	0.004	0.002	0.007

REFERENCES

[1] Marsico, Fabio; Paolillo, Stefania; Filardi, P. P. NSAIDs and cardiovascular risk. *J. Cardiovasc. Med.* **18**, e40–e43 (2017).

[2] Shaaban, M. A. *et al.* Design, synthesis, and biological evaluation of new pyrazoloquinazoline derivatives as dual COX-2/5-LOX inhibitors. *Arch. Pharm. (Weinheim).* **353**, (2020).

[3] Jacqueline K.InnesaPhilip C.Caldera. Omega-6 fatty acids and inflammation. *Prostaglandins, Leukot. Essent. Fat. Acids* **132**, 41–48 (2018).

[4] Meshram, M. A., Bhise, U. O., Makhal, P. N. & Kaki, V. R. Synthetically-tailored and nature-derived dual COX-2/5-LOX inhibitors: Structural aspects and SAR. *Eur. J. Med. Chem.* **225**, 113804 (2021).

[5] Shabaan, M. A., Kamal, A. M., Faggal, S. I., Elsahar, A. E. & Mohamed, K. O. Synthesis and biological evaluation of pyrazolone analogues as potential anti-inflammatory agents targeting cyclooxygenases and 5-lipoxygenase. *Arch. Pharm. (Weinheim).* **353**, (2020).

[6] Jaismy Jacob, P. & Manju, S. L. Novel approach of multi-targeted thiazoles and thiazolidenes toward anti-inflammatory and anticancer therapy—dual inhibition of COX-2 and 5-LOX enzymes. *Med. Chem. Res.* **30**, 236–257 (2021).

[7] Gaganpreet Kaur, O. S. Multiple target-centric strategy to tame inflammation. *Future Med. Chem.* **9**, 1361–1376 (2017).

[8] C.A.C.HydeS.Missailidis. Inhibition of arachidonic acid metabolism and its implication on cell proliferation and tumour-angiogenesis. *Int. Immunopharmacol.* **9**, 701–715 (2009).

[9] Gedawy, E. M., Kassab, A. E. & El Kerdawy, A. M. Design, synthesis and biological evaluation of novel pyrazole sulfonamide derivatives as dual COX-2/5-LOX inhibitors. *Eur. J. Med. Chem.* **189**, 112066 (2020).

[10] Jaismy JacobP,S.L.Manju, K.R.Ethiraj, G. Safer anti-inflammatory therapy through dual COX-2/5-LOX inhibitors: A structure-based approach. *Eur. J. Pharm. Sci.* **121**, (2018).

[11] S. Tries, W. N. & S. L. The mechanism of action of the new antiinflammatory compound ML3000: inhibition of 5-LOX and COX-1/2. *Inflamm. Res. Vol.* **51**, 135–143 (2002).

[12] Sabe, V. T. *et al.* Current trends in

computer aided drug design and a highlight of drugs discovered via computational techniques: A review. *Eur. J. Med. Chem.* **224**, 113705 (2021).

[13] Masand, V. H. *et al.* Does tautomerism influence the outcome of QSAR modeling? *Med. Chem. Res.* **23**, 1742–1757 (2014).

[14] David C. Young. *Computational Drug Design- A guide for Computational and Medicinal Chemists*. (Wiley Publications, 2009).

[15] Palacios, J. Computer Aided Design of Drug Delivery Systems.

[16] Oprea, T. I. On the information content of 2D and 3D descriptors for QSAR. *J. Braz. Chem. Soc.* **13**, 811–815 (2002).

[17] Vijay H.Masand, Nahed N.E.El-Sayed, Devidas T.Mahajan, Andrew G.Mercader, Ahmed M.Alafeefy, I. G. S. QSAR modeling for anti-human African trypanosomiasis activity of substituted 2-Phenylimidazopyridines. *J. Mol. Struct.* **1130**, 711–718 (2017).

[18] Yap, C. W. PaDEL-Descriptor : An Open Source Software to Calculate Molecular Descriptors and Fingerprints. *J. Comput. Chem.* **32**, 1466–1474 (2010).

[19] Gramatica, P., Chirico, N., Papa, E., Cassani, S. & Kovarich, S. QSARINS : A New Software for the Development , Analysis , and Validation of QSAR MLR Models. *J. Comput. Chem.* **34**, 2121–2132 (2013).

[20] Gramatica, P., Cassani, S. & Chirico, N. QSARINS-Chem : Insubria Datasets and New QSAR / QSPR Models for Environmental Pollutants in QSARINS. *J. Comput. Chem.* **35**, 1036–1044 (2014).

[21] Van de Waterbeemd, H. & Gifford, E. ADMET in silico modelling: Towards prediction paradise? *Nat. Rev. Drug Discov.* **2**, 192–204 (2003).

[22] Ntie-Kang, F. *et al.* In silico drug metabolism and pharmacokinetic profiles of natural products from medicinal plants in the Congo basin. *silico Pharmacol.* **1**, 12 (2013).

[23] Kitchen, D. B., Decornez, H., Furr, J. R. & Bajorath, J. Docking and scoring in virtual screening for drug discovery: Methods and applications. *Nat. Rev. Drug Discov.* **3**, 935–949 (2004).

[24] Xuan-Yu Meng, Hong-Xing Zhang, Mihaly Mezei, and M. C. Molecular Docking: A powerful

approach for structure- based drug discovery. *Curr. Comput. Aided Drug Des.* **7**, 146–157 (2012).

[25] Javed, M. A. *et al.* Structural Modification, in Vitro, in Vivo, Ex Vivo, and in Silico Exploration of Pyrimidine and Pyrrolidine Cores for Targeting Enzymes Associated with Neuroinflammation and Cholinergic Deficit in Alzheimer's Disease. *ACS Chem. Neurosci.* **12**, 4123–4143 (2021).

[26] Sajjad Ahmad, Mater H Mahnashi, Bandar A Alyami, Yahya S Alqahtani, farhat Ullah, Muhammad Ayaz, Muhammad Tariq, Abdul Sadiq, U. R. Blocks for Potential Analgesic Drugs: In vitro, in vivo and in silico Explorations. *Drug Des. Devel. Ther.* **15**, 1299–1313 (2021).

[27] Sadiq, A. *et al.* Tailoring the substitution pattern of Pyrrolidine-2,5-dione for discovery of new structural template for dual COX/LOX inhibition. *Bioorg. Chem.* **112**, (2021).

[28] Munir, A. *et al.* Synthesis, in-vitro, in-vivo anti-inflammatory activities and molecular docking studies of acyl and salicylic acid hydrazide derivatives. *Bioorg. Chem.* **104**, (2020).

[29] Jan, M. S. *et al.* Design, synthesis, in-vitro, in-vivo and in-silico studies of pyrrolidine-2,5-dione derivatives as multitarget anti-inflammatory agents. *Eur. J. Med. Chem.* **186**, (2020).

[30] Yap, C. W. PaDEL-descriptor: An open source software to calculate molecular descriptors and fingerprints. *J. Comput. Chem.* **32**, 1466–1474 (2010).

[31] Schrodinger Release 2021-1.

[32] Garrett M. Morris,Ruth Huey, A. J. O. Using AutoDock for Ligand-Receptor Docking. *Curr. Protoc. Bioinforma.* **24**, 8–14 (2008).

[33] Diego de Sousa Miranda. Python: a programming language for soware integration and development. *J Mol Graph Model* **17**, 57–61 (1999).

[34] Orlando, B. J. & Malkowski, M. G. Crystal structure of rofecoxib bound to human cyclooxygenase-2. *Acta Crystallographica Section:F Structural Biology Communications* vol. 72 772–776 (2016).

[35] Nathaniel C Gilbert, Sue G Bartlett, Maria T Waight, David B Neau, William E Boeglin, Alan R Brash, M. E. N. The structure of human 5-lipoxygenase. *Science (80-.).* **331**, 217–219 (2011).

[36] Guoli Xiong, Zhenxing Wu, Jiacai Yi, Li Fu, Zhijiang Yang, Changyu

Hsieh, Mingzhu Yin, Xiangxiang Zeng, Chengkun Wu, Aiping Lu, Xiang Chen, T. H. ADMETlab 2.0: an integrated online platform for accurate and comprehensive predictions of ADMET properties. *Nucleic Acids Res.* **49**, W5-w14 (2021).

[37] Phillips JC, Hardy DJ, Maia JD, Stone JE, Ribeiro JV, Bernardi RC, Buch R, Fiorin G, Hénin J, Jiang W, M. R. Scalable molecular dynamics on CPU and GPU architectures with NAMD. *J. Chem. Phys.* **153**, 044130 (2020).

[38] Yamada Y, Gohda S, Abe K, Togo T, Shimano N, Sasaki T, Tanaka H, Ono H, Ohba T, Kubo S, O. T. Carbon materials with controlled edge structures. *Carbon N. Y.* **122**, 694–701 (2017).

[39] G. Richard Bickerton, Gaia V. Paolini, Jérémy Besnard, S. M. & A. L. H. Quantifying the chemical beauty of drugs. *Nat. Chem.* **4**, 90–98 (2012).

[40] Christopher A.LipinskiFrancoLombardoBeryl W.DominyPaul J.Feeney. Experimental and computational approaches to estimate solubility and permeability in drug discovery and development settings. *Adv. Drug Deliv. Rev.* **23**, 3–25 (1997).

[41] Hughes, J. D. *et al.* Physiochemical drug properties associated with in vivo toxicological outcomes. *Bioorganic Med. Chem. Lett.* **18**, 4872–4875 (2008).

[42] Baell, J. B. & Holloway, G. A. New substructure filters for removal of pan assay interference compounds (PAINS) from screening libraries and for their exclusion in bioassays. *J. Med. Chem.* **53**, 2719–2740 (2010).

[43] Ertl, P. & Schuffenhauer, A. Estimation of synthetic accessibility score of drug-like molecules based on molecular complexity and fragment contributions. *J. Cheminform.* **1**, 1–11 (2009).

[44] Achutha AS, Pushpa VL, S. S. Theoretical insights into the anti-SARS-CoV-2 activity of chloroquine and its analogs and in silico screening of main protease inhibitors. *J. Proteome Res.* **19**, 4706–17 (2020).